CHAPTER 3

Modified Maximum Power Point Tracking Based-on Ripple Correlation Control and Sinusoidal Pattern Current Control for Single-phase VSI Grid-connected PV Systems

3.1 Introduction and outline

The single-phase single-stage VSI grid-connected PV systems has numerous advantages, such as simple topology, high efficiency, small size, low cost, etc. It needs to have an appropriate maximum power point tracking (MPPT) to continuously control the transferring maximum power from the PV array to the utility grid because of the characteristic of the PV power is nonlinear and time varying caused by changing of the atmospheric conditions [31]. Numerous MPPT techniques have been proposed for maximum power tracking such as hill-climbing, fractional open-circuit voltage control, perturb and observe (P&O), incremental conductance (IncCond), fractional short-circuit current control, fuzzy logic control, neural network, ripple correlation control (RCC) and several others. [24]–[27]. These techniques vary in complexity, sensors required, speed of convergence, cost, range of effectiveness, implementation hardware, popularity, and in other respects.

The RCC-MPPT method is the one which has the following features: very fast convergence to reach maximum power point MPP, parameter-insensitive MPPT of PV systems, several straightforward circuit implementations and well developed theoretical basis. It would be suitable for a modular application, which uses small converters and requires a high rate of convergence [2],[28]-[30]. In [29], the RCC-MPPT method is proposed by using the function of 1st order HPFs to generate the power ripple and voltage ripple from the measured PV power and PV voltage respectively, and using the

function of 1st order LPFs to avoid the ripple from the product of PV power ripple and PV voltage ripple. It can be used to control the MPPT for the single-phase VSI grid-connected PV systems. However it has some disadvantages about defining the suitable time constant of the filters to generate the desired output signal for correcting control. It also causes slow response, especially in case of rapidly shading irradiance.

In this thesis, a simple modified ripple correlation control (MRCC) MPPT method that produces a fast response RCC-MPPT and guarantees the correction of MPPT operating is proposed for single-phase single-stage VSI grid-connected PV system. Simulation results operated on the 928-kWp PV system show operating performance of the proposed MPPT method in 2 cases of all and partial rapidly shading irradiance.

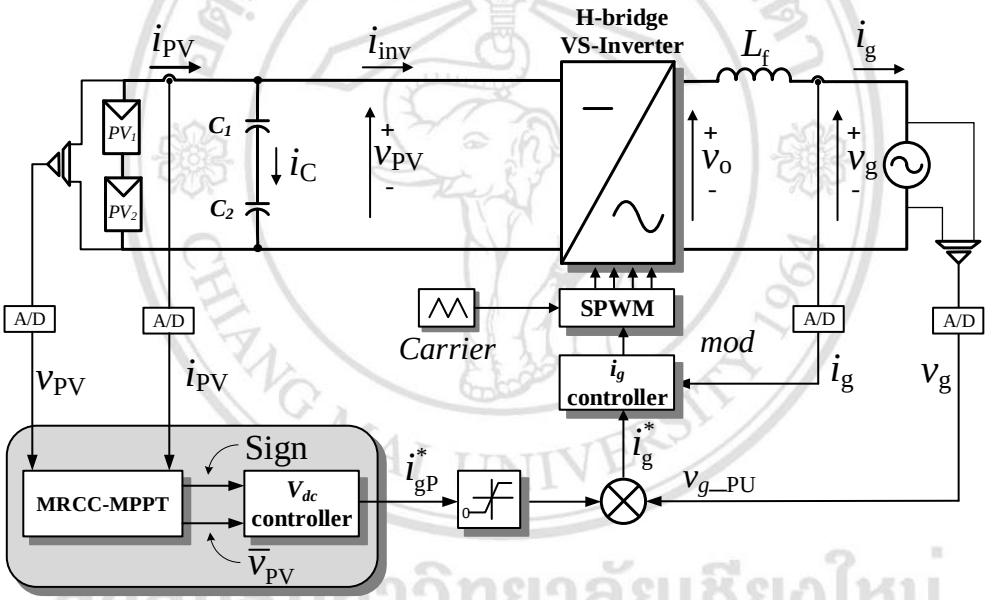

Figure. 3.1 The scheme of single-phase VSI grid-connected PV system.

3.2 Operating principle of the single-phase single-stage VSI Grid-connected PV systems

Figure 3.1 shows the scheme configuration of the single-phase single-stage VSI grid-connected PV system which has to handle at least 2 tasks, MPPT and injecting the sinusoidal grid current with unity power factor into the utility grid. The power scheme consists of three parts namely, a set of two series-connected PV strings for power feeding and supporting two cases of full and half rapidly shading irradiance, a set of two

series-connected decoupling capacitors which is parallel-connected to PV strings, and a buck type H-bridge VSI for converting the dc power to ac power which is injected to the utility grid through an inductor L_f. The control system consists of a sinusoidal pulse width modulation (SPWM) with unipolar technique for controlling the power switches of the inverter, a block of MRCC-MPPT for finding out the direction to reach the maximum power point (MPP) indicated by sign (-1,1), a dc-link voltage controller for regulating the PV voltage which follows the output of MRCC-MPPT by generating the peak current reference, and a grid current controller for control of injecting the sinusoidal grid current which is in-phase with respect to the grid voltage. The generation of the sinusoidal grid current i_g which is in-phase to the grid voltage v_g causes the oscillations in the instantaneous grid power with twice the line frequency 2ω as

$$p_g = P_{\text{grid}}.(1-\cos(2\omega t)) \tag{3.1}$$

where P_{grid} is the active power transferred to utility grid [2].

From Figure 3.1, the effect of the oscillation causes the instantaneous PV voltage v_{PV}, instantaneous PV current i_{PV} and instantaneous PV power p_{PV} to generate the oscillation in the same frequency as p_g. Because the instantaneous grid current i_g is related with the instantaneous PV current i_{PV} as $i_g = i_{\text{PV}} - i_C$, that means the two upper power switches in the H-bridge are in the opposite status, $S_1 \neq, S_3$. The instantaneous grid current $i_g = (S_1 - S_3)\cdot i_{\text{inv}}$ and the instantaneous output voltage of VSI $v_o = (S_1 - S_3)\cdot v_{\text{PV}}$ where $S_1, S_3 \in \{0,1\}$, are the status of two upper power switches of H-bridge VSI {OFF,ON}, the i_{inv} and v_0 the instantaneous input current and output voltage of H-bridge VSI, respectively. From these mentioned relationships, the instantaneous PV current i_{PV} can be written as

$$i_{\text{PV}} = \frac{i_g}{(S_1 - S_3)} + i_C \quad ; \; S_1 \neq, S_3 \tag{3.2}$$

where i_C is the instantaneous capacitor current. The equation of instantaneous PV voltage is given by

$$v_{PV} = \frac{v_L + v_g}{(S_1 - S_3)} \quad ; \; S_1 \neq S_3 \tag{3.3}$$

where v_L is the voltage crossing the inductor. The relationships of instantaneous PV power p_{PV} between instantaneous grid power p_g, instantaneous capacitor power p_C, and instantaneous inductor power p_L, when neglecting power losses in H-bridge VSI is given by

$$p_{PV} = p_C + p_L + P_{grid}(1 - \cos(2\omega t)) \tag{3.4}$$

The increase of the amplitude of PV voltage ripple $\hat{u}_{PV}$ inherent in the PV voltage v_{PV} at the PV array terminals causes lower power transferred to the utility grid. Reducing the amplitude of PV voltage ripple can be done by increasing the size of decoupling capacitor C_{dc} or the value of PV voltage V_{PV} as the relationship of following equation

$$\hat{u}_{PV} = \frac{P_{PV}}{2.\omega.C_{dc}.V_{PV}} \tag{3.5}$$

where p_{PV} is the nominal power of the PV array, V_{PV} is the mean of PV voltage and C_{dc} is the total capacitance of the series-connected C_1 and C_2 in the scheme in Figure 3.1 [2].

3.3 Analysis of the direct RCC-MPPT for the grid-connected PV system

3.3.1 Principle of the RCC-MPPT

Most of MPPT algorithms are based on the tracking of the maximum power operating point which is the minimum or zero derivative of the PV power with respect to the change in PV voltage. It can be written as $\partial p_{PV} / \partial v_{PV} = 0$. The derivative of PV power $\partial p_{PV} / \partial v_{PV}$ is an important value for MPPT process, its sign is used to indicate the direction of the MPP tracking by increasing or decreasing the reference PV voltage v_{PV}^* in the dc voltage controller. Figure 3.2 shows the four curves of PV characteristic, *i-v*

curve, *p-v* curve and power derivative $\partial p_{PV} / \partial v_{PV}$ curve, and the change in PV power. The desired MPP is on the top of *p-v* curve. From the characteristic of PV panel, the MPPT algorithm must force to move the operating point of PV system to operate on the MPP by regulating the PV voltage or PV current. In case of regulating the PV voltage for MPPT, the condition of tracking the MPP can be considered as the following conditions. If the operating point is in the left hand side of MPP, the power derivative $\partial p_{PV} / \partial v_{PV} > 0$ and the change in PV power $\partial p_{PV} > 0$ during the change in PV voltage $\partial v_{PV} > 0$, the PV voltage must be increased to approach the MPP. If the operating point is in the right hand side of MPP, the power derivative, $\partial p_{PV} / \partial v_{PV} < 0$ and the change in PV power $\partial p_{PV} < 0$ during the change in PV voltage $\partial v_{PV} < 0$, the PV voltage has to be decreased to reach the MPP.

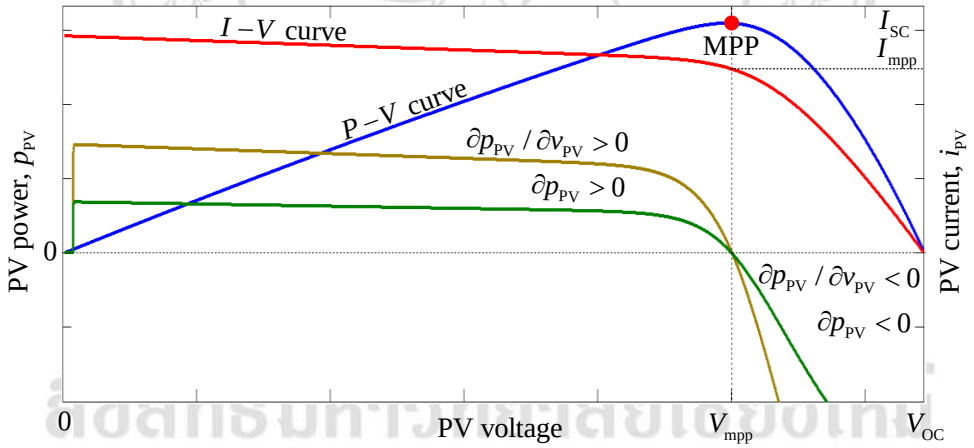

Figure 3.2 The PV characteristic P-V and I-V curves and the behavior of $\partial p_{PV} / \partial v_{PV}$ and ∂p_{PV} while the PV power is moved through the MPP in the STC.

In this study, the instantaneous PV power ripple $\tilde{p}_{PV}$ and the instantaneous PV voltage ripple $\tilde{v}_{PV}$, which are the inherent alternative components at the dc side of a single-phase single-stage VSI grid-connected PV system, are selected to represent the change in PV power ∂p_{PV} and ∂v_{PV}, respectively. Because the waveforms of the change in PV power ∂p_{PV} and the ripple of PV

power $\tilde{p}_{\text{PV}}$ is acted similarly when focusing on to indicate the MPP. In addition, for the calculation of power derivative $\partial p_{\text{PV}} / \partial v_{\text{PV}}$ or $\tilde{p}_{\text{PV}} / \tilde{v}_{\text{PV}}$, it has a chance to meet the problem about the infinity value if the change in PV voltage is met the zero $\partial v_{\text{PV}} = 0$ or $\tilde{v}_{\text{PV}} = 0$. To overcome this problem, To multiplies the PV voltage ripple $\tilde{v}_{\text{PV}}$ and calculating the average value for both upper and lower terms of the power derivative can be given as

$$\begin{aligned}
\left(\frac{\partial p_{\text{PV}}}{\partial v_{\text{PV}}}\right) &\cong \frac{\tilde{p}_{\text{PV}}}{\tilde{v}_{\text{PV}}} \cong \frac{\tilde{p}_{\text{PV}} \cdot \tilde{v}_{\text{PV}}}{\tilde{v}_{\text{PV}} \cdot \tilde{v}_{\text{PV}}} \\
&\cong \frac{\text{average of } (\tilde{p}_{\text{PV}} \cdot \tilde{v}_{\text{PV}})}{\text{average of } (\tilde{v}_{\text{PV}} \cdot \tilde{v}_{\text{PV}})} \\
&\cong \frac{\frac{2}{T}\int_{t-\frac{T}{2}}^{t} \tilde{p}_{\text{PV}} \cdot \tilde{v}_{\text{PV}} \cdot dt}{\frac{2}{T}\int_{t-\frac{T}{2}}^{t} \tilde{v}_{\text{PV}} \cdot \tilde{v}_{\text{PV}} \cdot dt} \\
&\cong \frac{\int_{t-1/2f}^{t} \tilde{p}_{\text{PV}} \cdot \tilde{v}_{\text{PV}} \cdot dt}{\int_{t-1/2f}^{t} \tilde{v}_{\text{PV}} \cdot \tilde{v}_{\text{PV}} \cdot dt} \cong \frac{\overline{\tilde{p}_{\text{PV}} \cdot \tilde{v}_{\text{PV}}}}{\overline{\tilde{v}_{\text{PV}} \cdot \tilde{v}_{\text{PV}}}}
\end{aligned} \tag{3.6}$$

To find out the power derivative, this method needs to know the oscillation frequency f_{OS} to receive the shortest period for average calculation. From the interested single-stage grid-connected inverter, the desired ripple frequency is made from the oscillation of the instantaneous grid power which is double the grid frequency f, $f_{\text{OS}} = 2f$ (see Figure 3.3(b)). In this case, the time period to calculate the average value of the both upper and lower terms of (3.5) is only 10 milliseconds.

Normally, the signal consists of two main components; ac and dc. The desired instantaneous ripple signal of PV power $\tilde{p}_{\text{PV}}$ and voltage $\tilde{v}_{\text{PV}}$ can be defined those are the ac components, which are given by

$$\begin{aligned} \tilde{p}_{\mathrm{PV}} &= p_{\mathrm{PV}} - \bar{p}_{\mathrm{PV}}, \\ \tilde{v}_{\mathrm{PV}} &= v_{\mathrm{PV}} - \bar{v}_{\mathrm{PV}}, \end{aligned} \tag{3.7}$$

where $\bar{v}_{\mathrm{PV}}$ and $\bar{p}_{\mathrm{PV}}$ are the dc components of PV voltage and PV power, respectively.

For example, from the scheme of a single-phase single-stage grid-connected PV system as Figure 3.1, its parameters are defined as Table 3.1. In Figure 3.3, the waveforms (a)-(h) present the behavior of the inherent variables in the single-phase single-stage H-bridge VSI for grid-connected PV system during the PV power p_{PV} is moved through the MPP by using the simulation results from Matlab Simulink. This happening is created by slight increasing of the grid current i_{g} until the operating point of PV power is moved through the MPP to expose the relationship of (3.1)–(3.5). The power injected to the grid p_{g} is always oscillated in double the grid voltage frequency (100 Hz). In this case, the grid voltage v_{g} and current i_{g} are in-phased or unity power factor, the instantaneous grid power p_{g} can be moved from zero (minimum) to twice the average active grid power P_{g} (maximum) following (3.1) as shown its waveform in Figure 3.3 (a)-(b). The PV voltage v_{PV} and PV current i_{PV} are continuously decreased and increased following the *P-V* and *I-V* characteristic curves of PV array while the grid current is moving up as shown in Figure 3.3 (c)-(d). The amplitude of PV voltage and current is always swung and out of phase each other with the same frequency as grid power frequency causing by charging and discharging of the decoupling capacitor C_1. The charging period is happened during the amplitude of PV voltage is increased from minimum to maximum and the grid power p_{g} is lower than the PV power p_{PV}. Otherwise, while the decoupling capacitor C_1 is discharging, the PV voltage is decreased from maximum to minimum and the grid power p_{g} is higher than the PV power p_{PV}. In Figure 3.3 (e) between 10-49 ms, the PV power p_{PV} is forced to be higher following the rise

of PV current i_{PV} until stable or the change in PV power is close to the zero $dp_{PV}/dt \cong 0$ while the PV power is met the MPP of PV array which is according to the *P-V* curve between the right hand side of MPP and the MPP (see Figure 3.2). In this period, the waveforms of PV power and voltage ripples are out of phase each other as presented in Figure 3.3 (f) affecting the multiplying result between them is lower than zero as shown in Figure 3.3 (g). After that, time between 49-75ms, the PV power is moved down to be lower than the MPP because its operating point is in the left hand side of MPP in the *P-V* curve. Also, the PV power and voltage ripples are in-phase providing multiplying result of them is higher than zero. The moving average value of those multiplying result are used to make the sign signal which is easier to decide which point is the MPP of PV array as shown in Figure 3.3 (h). From Figure 3.2 and 3.3, it is clear to indicate that:

- When the operating point is in the left hand side of MPP of *P-V* and *I-V* curves. The average value of the multiplying result between PV power and voltage ripples $\overline{\tilde{p}_{PV} \cdot \tilde{v}_{PV}}$ is over than zero and its sign is "+1". It means the PV voltage must be increased to approach the MPP.
- When the operating point is in the right hand side of MPP of *P-V* and *I-V* curves. The average value of the multiplying result between PV power and voltage ripples $\overline{\tilde{p}_{PV} \cdot \tilde{v}_{PV}}$ is lower than zero and its sign is "-1". It means the PV voltage must be decreased to approach the MPP.

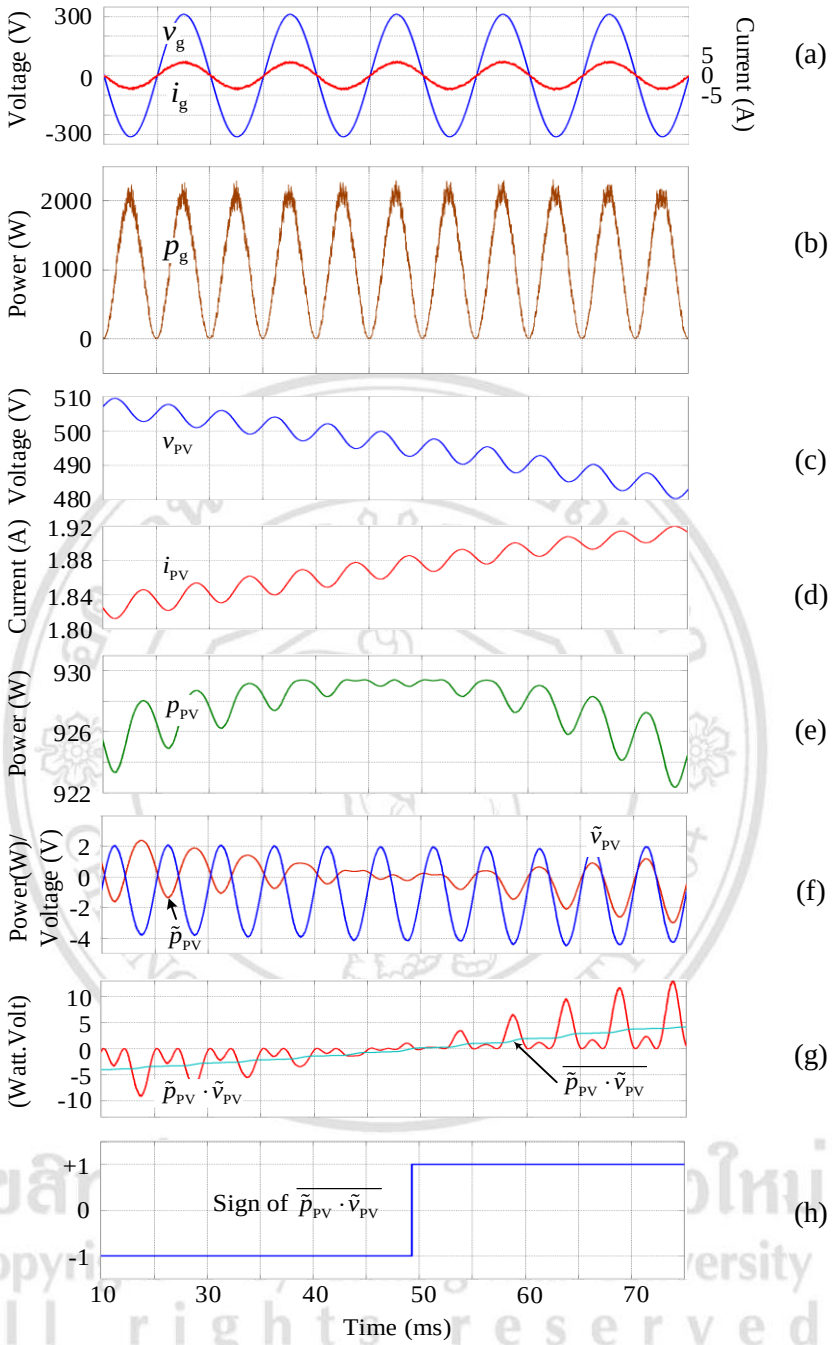

Figure 3.3 The behavior of variables in the single-phase single-stage grid-connected PV system with RCC-MPPT during the grid current is slightly increased to through the MPP of PV system, (a) grid voltage v_g and current i_g, (b) grid power p_g, (c) PV voltage v_{PV}, (d) PV current i_{PV}, (e) PV power p_{PV}, (f) ripple of PV power $\tilde{p}_{PV}$ and voltage $\tilde{v}_{PV}$,(g) product of $\tilde{p}_{PV} \cdot \tilde{v}_{PV}$ and its mean $\overline{\tilde{p}_{PV} \cdot \tilde{v}_{PV}}$, (h) sign of $\overline{\tilde{p}_{PV} \cdot \tilde{v}_{PV}}$.

3.3.2 A RCC-MPPT for the grid-connected PV system

In [29], a conventional RCC-MPPT (CRCC-MPPT) method is proposed to obtain the power derivative $\partial p_{PV} / \partial v_{PV}$ by using the function of 1st order high-pass filter (HPF) to calculate the instantaneous PV voltage ripple $\tilde{v}_{PV}$ and PV power ripple $\tilde{p}_{PV}$, and using the 1st order low-pass filter (LPF) instead the average function to obtain the dc component of multiplying result between the PV power and PV voltage ripples $\overline{\tilde{p}_{PV} \cdot \tilde{v}_{PV}}$, finally the sign of $\overline{\tilde{p}_{PV} \cdot \tilde{v}_{PV}}$ is generated by hysteresis component as shown in Figure 3.4. The instantaneous PV voltage ripple $\tilde{v}_{PV}$, PV power ripple $\tilde{p}_{PV}$ and the multiplying result of them are calculated as

$$\tilde{V}_{PV}(s) = \frac{\tau_{HPF}}{(\tau_{HPF} \cdot s + 1)} \cdot V_{PV}(s), \tag{3.8}$$

$$\tilde{P}_{PV}(s) = \frac{\tau_{HPF}}{(\tau_{HPF} \cdot s + 1)} \cdot P_{PV}(s), \tag{3.9}$$

$$\overline{\tilde{P}_{PV}(s) \cdot \tilde{V}_{PV}(s)} = \frac{\tilde{P}_{PV}(s) \cdot \tilde{V}_{PV}(s)}{\tau_{LPF} S + 1}, \tag{3.10}$$

respectively. It can be seen that, the proper two time constant values for HPF τ_{HPF} and LPF τ_{LPF} are required.

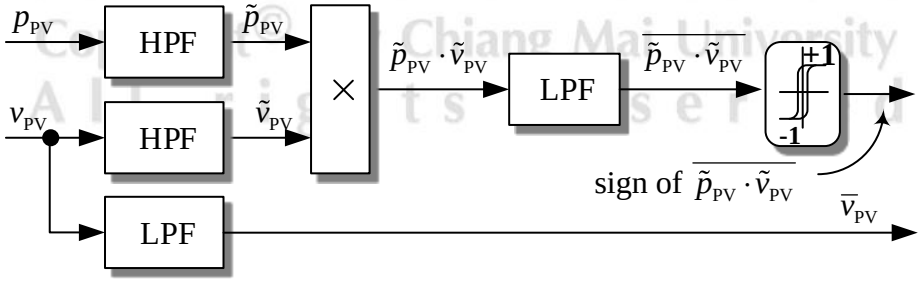

Figure 3.4 To obtain the PV power ripple $\tilde{p}_{PV}$, PV voltage ripple $\tilde{v}_{PV}$ and the conventional RCC-MPPT [29].

Although the HPF and LPF are easy to implement but they need the suitable time constant values τ_{HPF}, τ_{LPF} which can affect to the accuracy of the corrected MPP indicating. Figure 3.5 shows the effect of use the three difference time constant values of HPF function τ_{HPF} for extracting the inherent 3 Wp ripple from the PV power while is rapidly changed from 300W to 240W simulated by Matlab Simulink. From the results, the ripple produced by the HPF with $\tau_{\mathrm{HPF}} = 1\mathrm{ms}$ is the fastest response but its waveform is distorted from the reference ripple (Ripple Ref) leading to indicate the mistaken MPP. The waveform of ripple from HPF with $\tau_{\mathrm{HPF}} = 30\mathrm{ms}$ is resembled to the reference ripple but it is so slow to converge the desired ripple (120ms). The use of these time constant values affects to the accuracy of the MPP indicating as shown in Figure 3.8. Furthermore, the sign signal (sign) has to be sent to the integrator block through the *K* constant in order to generate the dc voltage reference v_{PV}^{*}. The measured PV voltage v_{PV} used to subtract from dc voltage reference v_{PV}^{*} must be the dc component $\bar{v}_{\mathrm{PV}}$ (without the ripple or ac component) [18]. Because if the inherent 100 Hz ripple in PV power and voltage is transferred to the dc voltage controller as the measured values, it affects to degrade the quality of current injected to grid by inserting the 3rd harmonic to the grid current [18]. In this case, the filter block is required to eliminate the ac component out from the measured PV voltage v_{PV} to obtain the dc component $\bar{v}_{\mathrm{PV}}$ and is sent to the block of dc voltage controller.

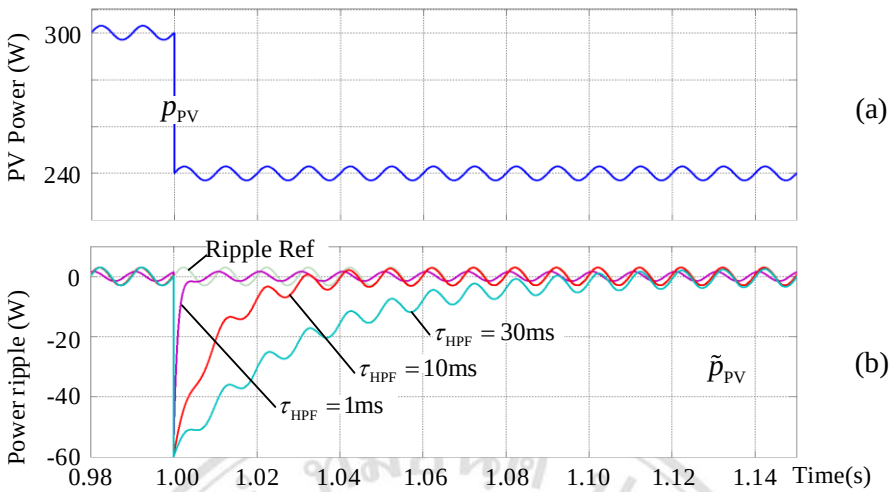

Figure 3.5 PV power ripples $\tilde{p}_{PV}$ extracted from PV power with the HPF functions during rapidly changing of PV power, (a) PV power p_{PV}, (b) PV power ripples $\tilde{p}_{PV}$ produced by HPF with three difference time constant values $\tau_{HPF} \in \{1\text{ms}, 10\text{ms}, 30\text{ms})\}$.

3.4 Modified RCC-MPPT for the grid-connected PV system

According to the principle of RCC-MPPT method, it is well-known that the accuracy of the RCC-MPPT depends on the correcting of the desired ripples $\tilde{v}_{PV}$, $\tilde{p}_{PV}$. To obtain the PV power and voltage ripples $\tilde{v}_{PV}$, $\tilde{p}_{PV}$ as (3.6), the desired ripples can be achieved by eliminating the dc component from the input signal. This method has some advantage as follow

- Easy to implement.
- There is no need to define the suitable time constant value for obtaining the corrected ripple waveform as the use of HPF and LPF functions,
- The existed dc component of PV voltage $\bar{v}_{PV}$ can be the measured PV voltage used in the dc voltage controller, thus the proposed MRCC-MPPT needs no filter for removing the ac component as the conventional RCC-MPPT.

Therefore, the modified RCC-MPPT (MRCC-MPPT) proposes the use of moving average (MA) function for generating the dc component or the average value, and then that dc component is eliminated from the input signal to obtain the required ripple

signal. In addition, the minimum time period to calculate the right dc component is depended on one cycle time period of desired ripple which has only 10 millisecond as one cycle time period of the instantaneous grid power p_g. Figure 3.6 illustrates the block diagram of the proposed modified RCC-MPPT technique to find out the sign signal based on (3.6) and to extract the ripples from the instantaneous PV power and voltage based on the MA function as (3.7).

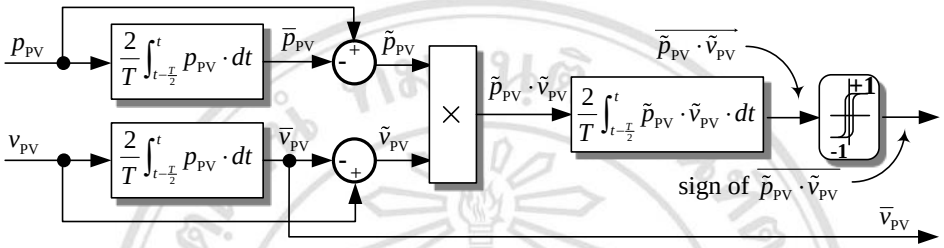

Figure 3.6 Block diagram of the proposed modified RCC-MPPT.

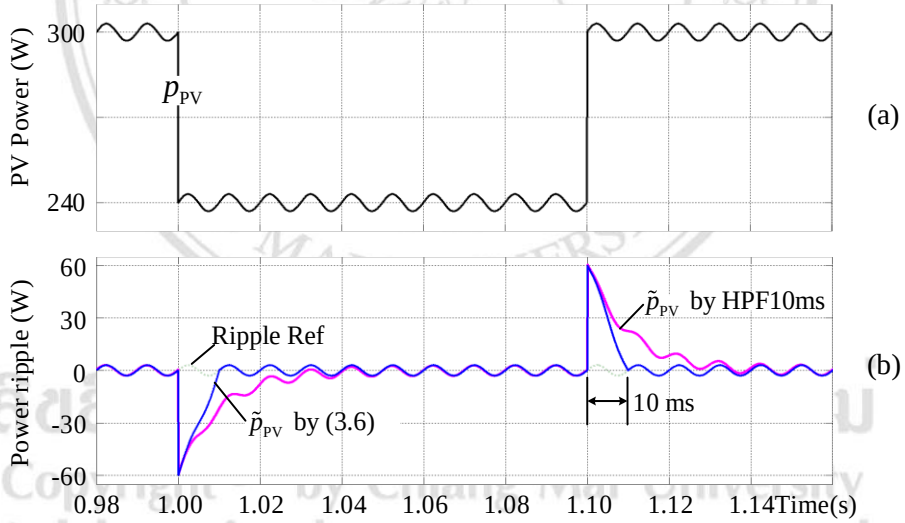

Figure 3.7 To compare the convergence speed of extracting the PV power ripples $\tilde{p}_{PV}$ from PV power p_{PV}, (a) PV power p_{PV}, (b) PV power ripples $\tilde{p}_{PV}$ produced by HPF function (pink) and following (3.7) based on MA function (blue).

Figure 3.7 shows the comparison of convergence speed to extract the desired ripple $\tilde{p}_{PV}$ from PV power p_{PV} between the use of HPF with $\tau_{HPF} = 10\text{ms}$ and the moving average functions for calculating the dc component applied in (3.6). It can be seen that

the ripple signal produced by (3.7) based on the moving average function is faster to converge the pure ac component after the PV power is rapidly changed from 300W to 240W and from 240W to 300W.

Figure 3.8 shows the comparison between the simulation result of the sign signal made by the conventional RCC-MPPT based on the HPFs and LPF and the sign signal made by the modified RCC-MPPT based on the MA function. Both methods are operated in the same condition and PV system parameters shown in Table I, except use of MPPT algorithm. From the results, it can be seen that the sign signal produced by the MRCC-MPPT can indicate the exact MPP more accurate than the sign signal from the CRCC-MPPT in case of the time constant values used in the HPFs $\tau_{\text{HPF}} = 10\text{ms}$ and LPF $\tau_{\text{LPF}} \in \{5\text{ms}, 10\text{ms}\}$ are selected.

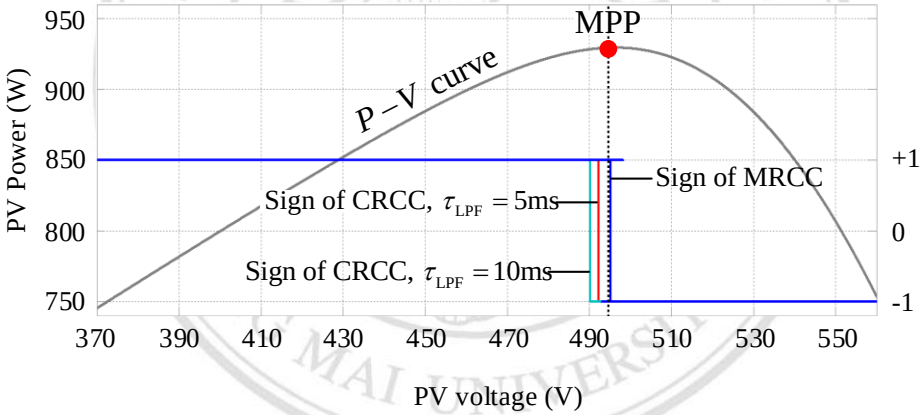

Figure 3.8 Comparison between the sign signal made by the MRCC (blue), the CRCC with $\tau_{\text{LPF}} = 5\text{ms}$ (red), and the CRCC with $\tau_{\text{LPF}} = 10\text{ms}$ (green).

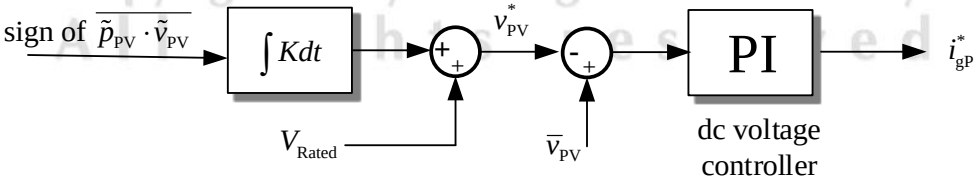

Figure 3.9 Block diagram of voltage reference generating and dc voltage controller

Figure 3.9 shows the block diagram of the dc voltage controller including the linear integral through a constant K and plus with the rated maximum power point voltage V_{Rated} of the PV array to generate the dc voltage reference v^*_{PV} which can be given by

$$v_{PV}^{*} = V_{mpp} + [\text{sign of } \overline{\tilde{p}_{PV} \cdot \tilde{v}_{PV}}] \cdot K \int dt, \tag{3.11}$$

when the V_{Rated} is the MPP voltage in the standard test condition (STD) defined by the producer. The convergence speed of the MPPT of the control system is depend on the constant *K*. The proportional and integral (PI) dc voltage controller is selected to compensate the error by generating the reference peak grid current i_{gP}^{*}.

In order to inject the power to grid with high performance under the condition of the interconnections of PV systems to grid standard such as IEC61720, IEEE1547, and EN61000-3-2. The current injected to the grid have to be controlled with fast responding. The dynamic function of the current injected to the grid is considered in the ac side of GCPVS based on the Kirchhoff's voltage law. Figure 3.10 shows the block diagram of the current control loop. The PI type of controller is used to compensate the error from the different value between the sinusoidal grid current reference i_{g}^{*} and the measured grid current i_{g}, the output of PI type current controller is the modulation signal *mod* used to generate the sinusoidal pulse width modulation (SPWM) controlled with the unipolar technique [32].

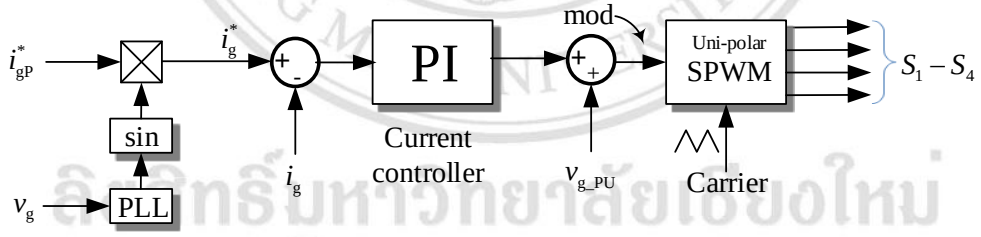

Figure 3.10 Block diagram of the current controller and the SPWM gate drive signals.

Table 3.1 Main designed parameters of PV system

Parameters	Symbol	Value
PV panel		
Short-circuit current in STC1	I_{sc}	1.12 A
Open-circuit voltage in STC	V_{oc}	85 V
MPP voltage in STC	V_{mpp}	63 V
MPP current in STC	I_{mpp}	0.92 A
PV array		
Rated current	I_{rated}	1.84 A
Rated MPP voltage	V_{rated}	504 V
Rated maximum power	P_{rated}	928 W
DC-link capacitor	C_1, C_2	2200µF, 400Vdc
Power and control scheme		
PWM carrier frequency	f_{sw}	14 kHz
Single-phase utility grid	V_g, f_1	220 Vrms, 50 Hz
Inductor	L_f	5 mH
dc link voltage controller: PI	K_p	0.4
	K_i	15
Grid current controller: PI	K_p	0.05
	K_i	200

3.5 Simulation results

The PV system structure and control scheme shown in Figure 3.1 has been implemented in MATLAB/SIMULINK program in order to verify the behavior of the proposed MRCC-MPPT control. The model of the PV array based on the single-diode model, considering the characteristic of the cells and equations were implemented according to [33]. The PV source of this system is a PV array which consists of 16 PV panels. The parameters of each PV panel and PV system are shown in Table I. In order to verify the effect of the PV system using MRCC-MPPT in the situation of rapidly shading irradiance, it's defined to have two cases of irradiance changing. In case 1, all PV

panels in the array are shaded from irradiance in the same time (all shading) with moving down from 1000 to 500 W/m^2 and up from 500 to 1000 W/m^2 as shown in Figure. 3.12 (a). And in case 2, just 50% of the PV array are under shading condition with the same sequence of change as the case 1 (half shading), and the other are operated in constant irradiance as shown in Figure. 3.14 (a). In both cases, the irradiance changing is operated in 0.1 s period for the decreasing and increasing ramps. The irradiance starts from 1000 W/m^2 to 500 W/m^2, waits at this level for 0.9 s, and increases again from 500 W/m^2 to 1000 W/m^2 with a constant slope. The temperature is considered at 25°C constant during the simulation.

Figure 3.12 shows the simulation results of the proposed MRCC-MPPT method in case 1 studying, i.e. all shading irradiance. Figure 3.14 shows the simulation results of the proposed MPPT method in case 2, i.e. half shading irradiance. Figure 3.11(a) and Figure 3.13 (a) show the relationship curve between PV power p_{PV} versus PV voltage v_{PV} in case 1 and case 2, respectively. From these figures, it can be seen that the proposed MRCC-MPPT technique can track the MPP in both cases perfectly. Figure 3.11(b) and Figure 3.13 (b) show the relationship curve between PV current i_{PV} versus PV voltage v_{PV}. The curves are started from the minimum PV power point at point (A) and track to the MPP at point (B) following the line of P-V and I-V characteristic curves of the irradiance 1000 W/m^2. The PV power p_{PV} can be controlled to run around the MPP (928W) until the irradiance profile is reduced from 1000 to 500 W/m^2. It caused the PV power p_{PV} of both cases are reduced to operate around the new MPP at point (C).

In case 2, as shown in Figure 3.13, one half of PV panels are shaded which cause the MPP in this case is higher than the MPP in case 1. This led to the PV power in case 2 is higher than in case 1 also. The irradiance profile waits in this level 0.9 s and moved back to the last level (1000W/m2) again. It causes the PV power p_{PV} of both cases to increase and run around MPP (928W) immediately. From the mentioned results, it can be seen that the MPP of the PV system can be tracked immediately by the proposed MPPT method in both cases.

Figure 3.14 shows the behaviors of PV system variables controlled with the proposed method in case 2. The PV power is the summing of the capacitor power p_C and the injected power to inverter. Therefore the power transferred to utility grid comes from the input power of inverter multiplied with the modulated function of VSI. Figure 3.12(b) and Figure 3.14(b) show that the PV system can transfer most of the input power of inverter into the utility grid for both all shading and half shading cases, respectively.

Figure 3.12(d) and Figure 3.14(d) show the grid current waveform of case 1 and case 2, respectively. It can be seen that the proposed PV system can feed the sinusoidal current in-phase with grid voltage v_g, providing unity power factor of the utility grid.

3.6 Conclusion

This study has presented a MRCC-MPPT method by using the mean function to be the main process of control for single-phase single-stage VSI grid-connected PV system. From the results, it can be seen that the proposed algorithm causes higher accuracy for correction of the MPP and faster response compared with the used of the 1st order HPFs and LPF algorithm in the case of rapidly shading irradiance based on the same shape of desired ripples. The proposed method can generate the sinusoidal grid current with unity power factor. Furthermore, it can reduce a harmonic filter in the dc-link voltage controller. Simulation results confirm the correctness and reliability of the developed control scheme and algorithm with two situations of full and half PV string shading.

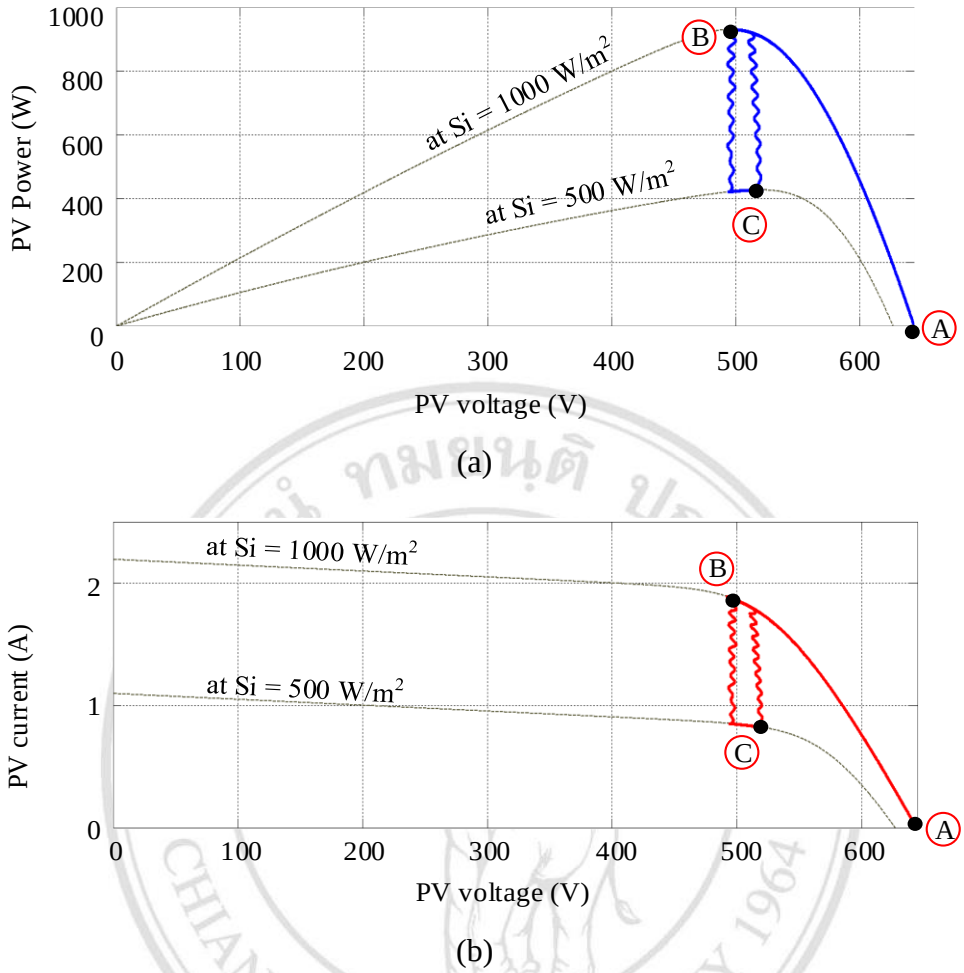

Figure 3.11 Relationship curve in case 1 between PV power p_{PV} versus PV voltage v_{PV} (a) and PV current i_{PV} versus PV voltage (b).

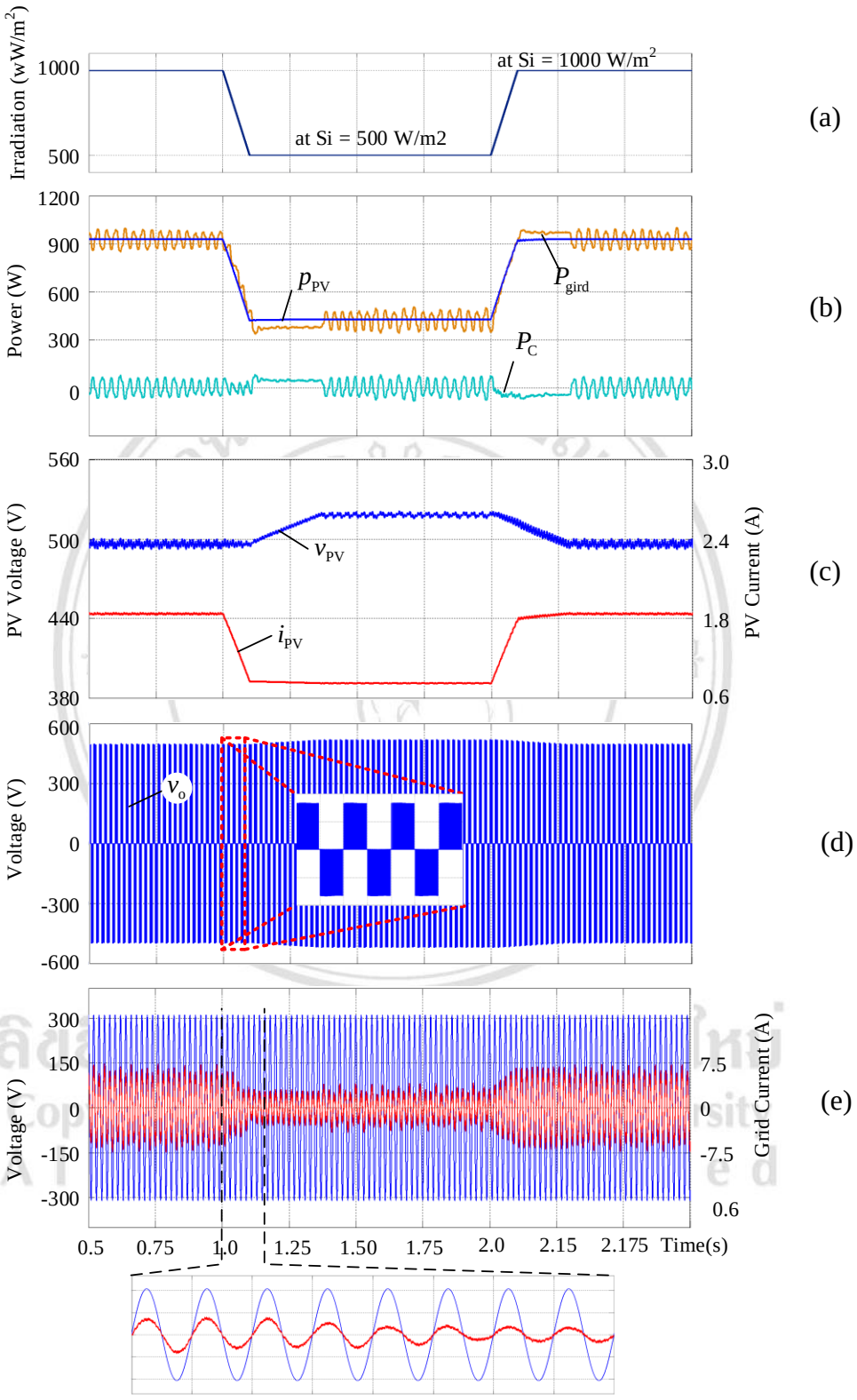

Figure 3.12 Behavior of variables in the grid-connected PV system controlled with the proposed MRCC-MPPT and simple grid current control in case 1(all PV array shading).

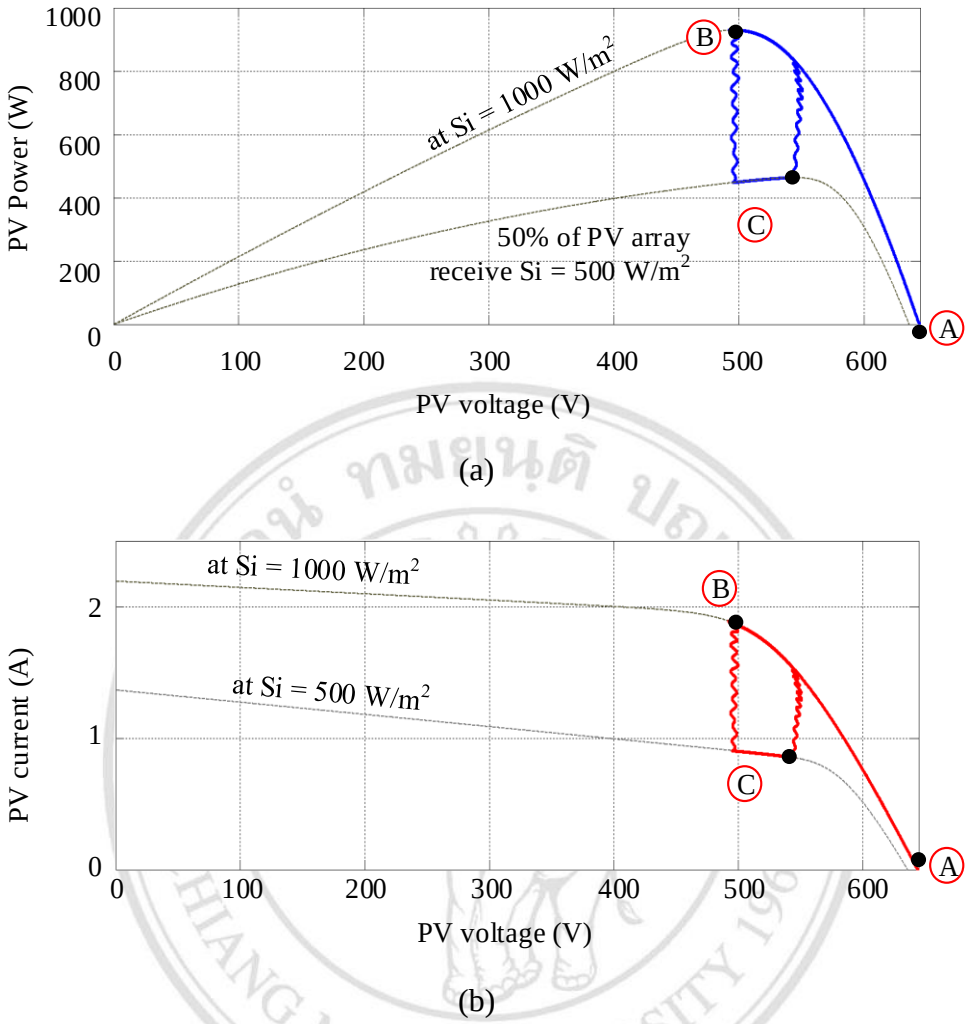

Figure 3.13 Relationship curve in case 2 between PV power p_{PV} versus PV voltage v_{PV} (a) and PV current i_{PV} versus PV voltage (b).

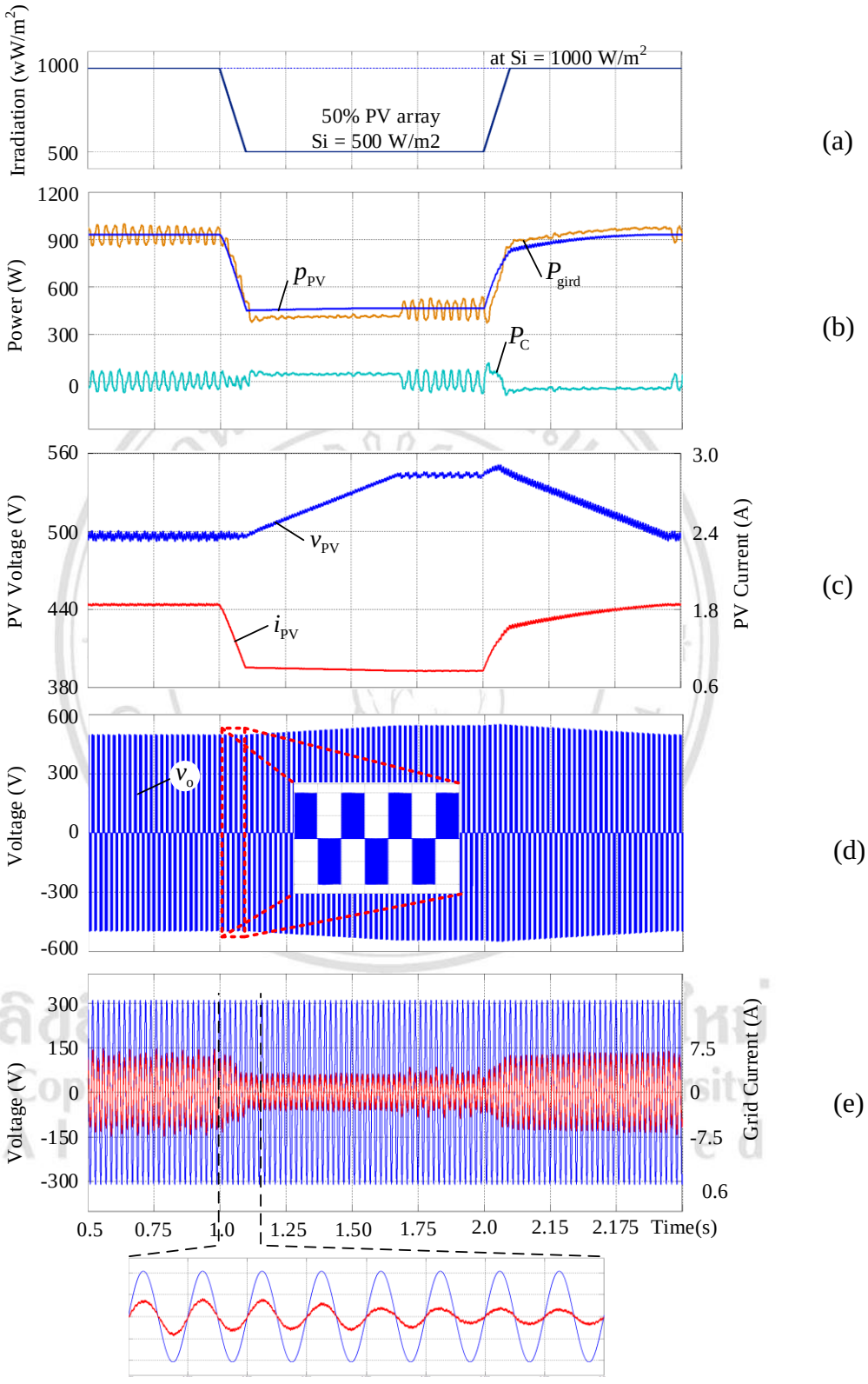

Figure 3.14 Behavior of variables in the grid-connected PV system controlled with the proposed MRCC-MPPT and simple grid current control in case 2 (50% PV shading).